RESEARCH PAPER

Broadband Damping Properties of Particle Dampers Mounted to Dynamic Structures

A. Schönle[1] · C. Gnanasambandham[1] · P. Eberhard[1]

Abstract

Background The background of this work is the classification of the broadband properties of particle dampers (PDs). This broadband characteristic has experienced little systematic investigation in experiments.

Objective So the primary objective of this paper is to find a measure to quantify the broadband damping properties of PDs. Also the demonstration of applicability to technical structures is a desired goal and the experiments provide a sound basis.

Methods The methods for evaluating the performance of particle dampers and tuned mass dampers target the reduction of vibration amplitudes over the frequency range. The test bench consists of a mechanical frame structure with multiple eigen-freqencies up to 200 Hz harmonically excited with an electrodynamic shaker. From the differences in the dynamic behaviour the performance metric will be derived and evaluated.

Results As a result, a dynamic structure is set up as an effective test bench for different damper configurations. Differences of the tested concepts in regard to the dynamic behaviour over a wide frequency range are observed. From the experimental data a performance metric is deduced to quantify these differences.

Conclusion The conclusions drawn from this paper are, that PDs provide high damping over a wide frequency range. Furthermore, with a suitable performance metric this broadband damping properties can be quantified for the use in further development of PDs.

Introduction

Particle dampers (PDs) and tuned mass dampers (TMDs) have shown to be beneficial to reduce undesired vibrations in technical systems. Improving the performance of a vibroimpact damper mounted on a beam through the usage of many particles in a bean bag was proposed in [1]. Further studies on a similar experimental setup were performed in [2] and an elementary analytical model for the PD was developed. The performance of a PD and the parameters influencing it have later been subject to numerous experimental and numerical investigations. Various experimental investigations showed the manifold parameters influencing the performance of PDs. A more extensive

study on particle materials, sizes, and mass ratio on a cantilever beam was conducted in [3]. Also the combination of particles and liquid in a PD was analysed in experiment and numerical simulation in [4]. In addition [5] studied the filling ratio, [6] showed the influence of the particle surface through simulation and experiment, in [7] the depth to diameter ratio for the PD cavity was investigated under various excitation levels. Complex shapes like tetrapods in addition to liquids as filling for PDs were considered in [8] and have proven great benefit through simulation and experiment. Elaborate experiments were performed in [9] to eliminate the effect of gravity on particle damping. In addition a broad review on different approaches on PDs was given in [10]. The current literature shows the manifold influences on PD performance. These influencing parameters, combined with the highly nonlinear behaviour of PDs still hinders their applicability. Particle movement in vertically vibrating PDs was studied for different excitation frequencies and amplitudes, e.g., in [11]. There, a

✉ P. Eberhard
   peter.eberhard@itm.uni-stuttgart.de

1   Institute for Engineering and Computational Mechanics,
    Pfaffenwaldring 9, 70569 Stuttgart, Germany

damping contour plot was used to analyse the PD behaviour under different moving conditions of the particles. In [12] an approach was presented to combine two different strategies of PD analysis. This includes namely the focus on the particle movement leading to energy dissipation and the general influence of a PD to its host structure. The beneficial effects for vibration problems in different scales and under different conditions was seen. However, most of the experiments in the mentioned literature use relatively simple host structures like a cantilever beam. To ensure adequate transferability of the obtained results, here a more sophisticated structure is of interest. Also for practical application a systematic design procedure is desirable. Great potential to fulfil this task can be found in experimentally validated numerical simulations as shown in [13]. This gives the ability to test various parameters independently without the need for an elaborated experimental setup during the design process. In order to achieve these goals, a test bench suitable for validation is necessary. A main requirement is, to ensure transferability of the gained insights to a wide range of structures in practice. Generalisation is more difficult, the more a structure serves a specific task. At the same time, a basic setup may neglect some effects relevant for practical application. This calls for realistic and complex dynamics in the frequency domain far exceeding that of a single degree of freedom system (SDOFS) as introduced in [7], but not as specific as for instance given in [14].

The desire for optimisation of particle dampers through simulations leads to the need for quantification of PD properties. One of these is the frequency depending damping characteristics. Statements on this attribute can often be found in literature, as for example in [5, 14] or [15]. This property is especially interesting, as the ability to cover a wide frequency range increases applicability significantly. Therefore, a structured investigation of the broadband damping characteristic of a PD is of great interest. Especially some kind of performance metric seems desirable for numerical optimisation. To derive such a performance metric from experimental data, devices with significantly different properties are to be examined.

In literature comparisons of different damping devices with a PD can be found. A TMD was compared to a PD for a SDOFS in [16]. A well structured detailed analysis for various excitation methods was performed in [17]. With a different setup, as a suspended pendulum on a SDOFS, a comparison of TMD and PD was performed in [18]. From such promising results the motivation for further studies is drawn. These investigations still lack a structure with multiple eigenfrequencies and a suitable quantification of the broadband damping properties. So in particular extending this comparison for a wider frequency range and in the process investigating the broadband damping
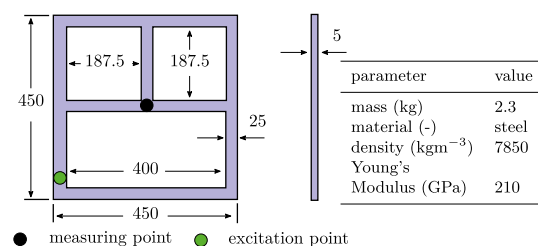
characteristics seems promising to achieve the motivated research goals.

The novel contribution of this paper is an experimental comparison of PDs and TMDs for a structure with multiple eigenfrequencies over a relatively wide frequency range. This paper is organized as follows: In "Experimental Setup" the experimental setup is described and in "Experimental Results" some experimental results are presented. The paper ends in "Conclusion" with some conclusions.

Experimental Setup

To study the broadband damping properties of a PD, a weakly damped frame structure as shown in Fig. 1 is designed. This frame structure exhibits multiple vibration modes even in the lower frequency range. When excited with a shaker, the frequency response of the host structure with a PD allows a systematic investigation of the broadband damping effect of PDs. The central aspect of the experimental setup, as shown in Fig. 2, consists of the weakly damped host structure of dimensions shown in Fig. 1. Also the locations of the forcing point (input) and the velocity measuring point (output) at the host structure are given. In Fig. 3, the lab setup used for the experiments is shown. The host structure is suspended by kevlar cords to replicate a free-free boundary condition. This gives the opportunity to study the dynamics of the structure independently from clamping to a surrounding suspension. To aid quick setup changes and to improve repeatability of the measurements, hooks as shown in Fig. 4(a) are provided. Moreover, the hooks are covered with rubber tubing to provide some vibration reduction between the host structure and the surrounding support structure.

The host structure is excited using an electromagnetic shaker, which is driven by a power amplifier Brüel & Kjær Type 2706. The driving signal for the shaker is controlled using a Tectronix AFG2022B signal generator. A PCB 288D01 impedance sensor situated between the shaker and the host structure is used to measure the force and acceleration at the forcing point (input). The forces and accelerations

parameter	value
mass (kg)	2.3
material (-)	steel
density (kgm^{-3})	7850
Young's Modulus (GPa)	210

● measuring point ● excitation point

Fig. 1 Geometry and dimensions of the host structure. All dimensions in mm

Fig. 2 Schematic representation of the forced vibration experimental setup used to systematically analyse the multi frequency damping properties of PDs
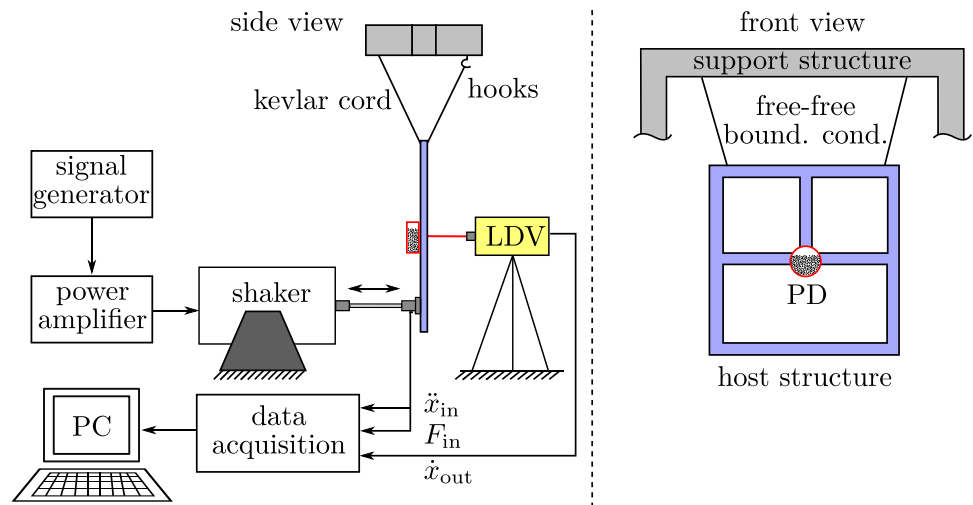

at the input vary, but are in a range up to 55 N and 40 ms^{-2} peak values, respectively.

The shaker is coupled to the host structure using an elastic stinger and a magnet, see Fig. 4(c). The stiffness of the stinger is carefully chosen to provide an optimal coupling between the shaker and the host structure and thereby improve the repeatability of the measurements. The velocity of the structure at the measuring point (output) is measured using a Polytec VibroGo-200 Laser Doppler Vibrometer. A transient-data recorder OROS OR35

real-time multi-analyser is used to record the experimental data and Matlab is used to perform the post processing.

To couple damping devices to the host structure, an adapter plate is build, see Fig. 4(b). This is then bonded to the host structure by applying a thin layer of two-part epoxy which can be separated by heat. Using this technique, the damping device can be mounted anywhere on the host structure by simply moving the adapter plate to a desired location and repeating the bonding procedure.

Fig. 3 Lab apparatus consisting of the host structure hung using kevlar cords. The host structure is excited using an electrodynamic shaker. A Laser Doppler Vibrometer is used to measure the structural response. A close-up view of the red boxes can be seen in Fig. 4
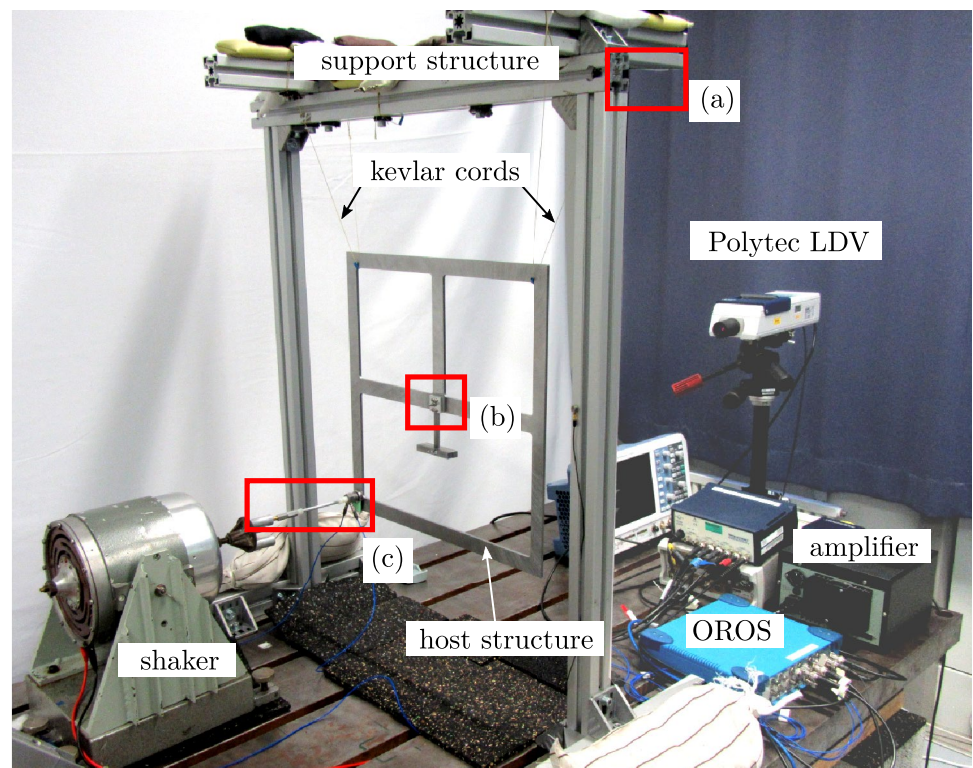
Fig. 4 Experimental enhancements to improve the quality of measurements. (**a**) Cup hooks with rubber isolation tubing for quick setup changes and better repeatability. (**b**) Two-part epoxy bonded adapter plate for flexible mounting of damping devices. (**c**) Suitably stiff stinger for optimal coupling between shaker and host structure
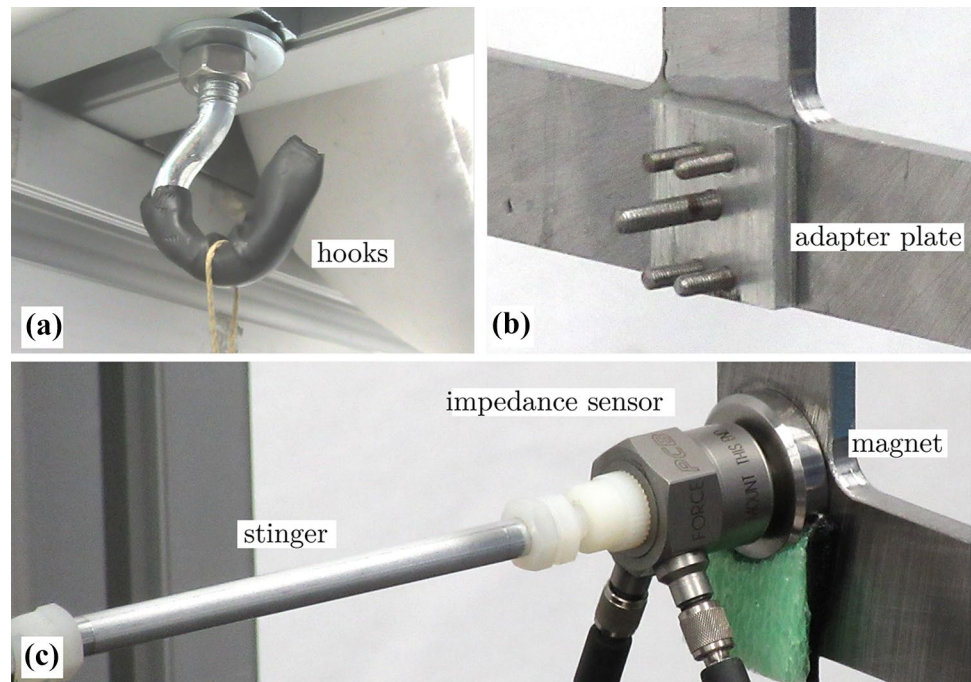
Experimental Results

Frequency Response of the Host Structure

First the frequency response of the host structure without any damper device is measured. The force signal is measured using the impedance sensor and the velocity signal is measured using the LDV. As the velocity characterizes the kinetic energy the mobility of the structure is an adequate representation for its dynamical behaviour. In addition, using signals that are directly measurable with high precision reduces potential sources of error. The corresponding experimental frequency response is shown in Fig. 5.

The first five response peaks are observed at 53 Hz, 62 Hz, 83 Hz, 128 Hz and 136 Hz. Similarly, the first 5 natural frequencies predicted using finite element analysis (FEA) are 51.2 Hz, 61.5 Hz, 80 Hz, 121 Hz and 134 Hz. This demonstrates a reasonable agreement between numerical analysis and experiment. It is also clearly seen that from the first five frequencies the frequencies at 62 Hz and 83 Hz are dominant. This is because at these frequencies the measuring point lies at a vibration antinode. This fact is clearly seen in the corresponding mode shapes predicted from FEA, see Fig. 5. Similarly, at 53 Hz, 128 Hz and 136 Hz, the host structure exhibits natural frequencies where the measuring point lies at a vibration node, see Fig. 5.

It is clearly seen that the measuring point for the 2nd natural frequency shows a very high response. As a consequence, the measuring point, for this particular mode shape, exhibits large displacements for small input forces,

thus making it an ideal location for mounting a PD as it promotes vigorous collisions and friction between the particles. For the following investigations, the PD is mounted at a location as shown in Figs. 2 and 6(b). At the mounting point of the PD the structure only exhibits horizontal movement. Subsequently, the effects of rotation of the PD or movement in the direction of gravity can be neglected.

Investigated Damper Configurations

In order to understand the broadband damping behaviour better, the damping performance of a PD is compared with that of a tuned mass damper (TMD). As the TMD only attenuates the vibration amplitudes for a small frequency band around the tuning frequency, it has only very limited broadband damping behaviour in contrast to a PD with better applicability over wider frequency ranges. These differences in the damping characteristics are here examined systematically and described through performance metrics. This provides numerical access to the broadband damping behaviour of such devices based on numbers and facts instead on impressions alone. Here, a design frequency of 60 Hz is chosen for the TMD because the host structure exhibits an antinode at the measuring point at this particular frequency. Moreover, to provide a fair comparison between PD and TMD, the total mass of the corresponding device is set to be 134 g each, which represents about 6 % of the total mass of the host structure. In addition to the two damper configurations, for comparison a third configuration is included in which a ballast mass (BM) of 134 g is attached to the host

Fig. 5 Experimental frequency response of the host structure (reference) without any damper device. The corresponding mode shapes are obtained using finiteelement analysis
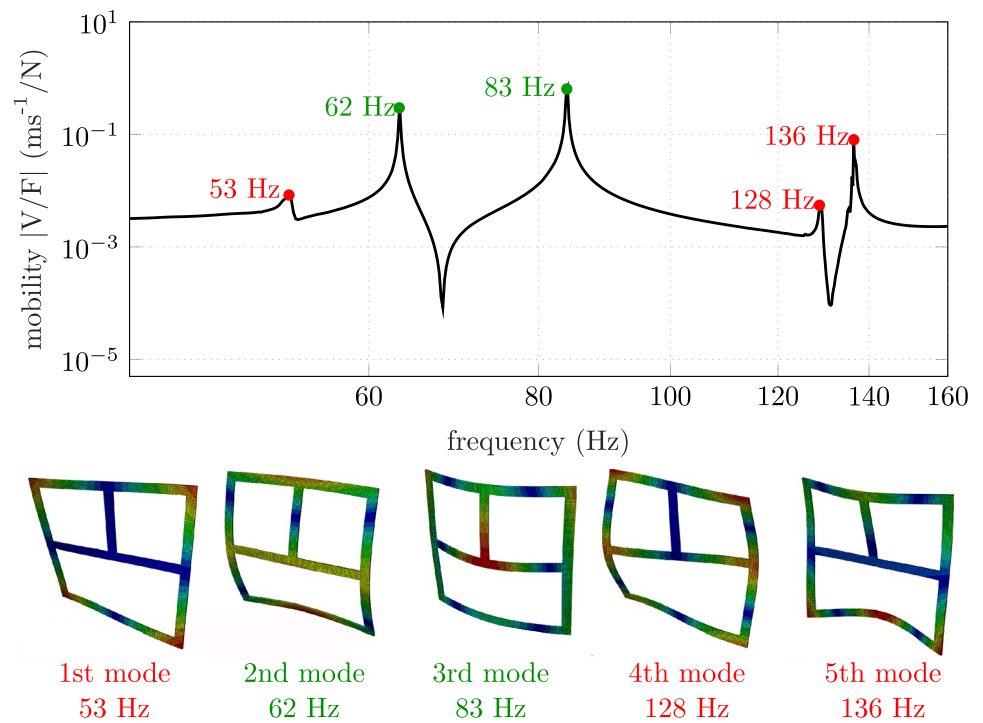

structure. This is done to compensate the effect of added mass intrinsically introduced by the damping devices.

Considering the mentioned design parameters, an optimal tuned mass damper is designed according to the procedure outlined in [19]. The corresponding TMD consists of a dynamic mass of 90 g attached to a long beam (58 mm x 12 mm x 2 mm) using screws. The length of the thin beam L and in turn the tuning frequency of the TMD can be varied during the experiments, see Fig. 6(a). The resulting parameters for the TMD are specified in Table 1.

The investigated particle damper is proposed for the design frequency of 60 Hz and a vibration amplitude of 1 mm. To design an optimal PD cavity, several simulations similar to the ones performed in [20] are carried out but

should not be described here. The total mass of the PD is mainly governed by the mass of the particle filling. In combination with the expected weight of the container this determines the number of particles of a given diameter. The influence of the particle diameter is investigated in [3] and it is suggested there that for a given mass using more particles with smaller diameter provides often better damping. The diameter of the PD container was chosen to achieve a compact PD with moderate filling ratio of about 60 %. This value was selected from previous experience. On the other hand, variation of the container length and evaluation of the damping properties by simulation provides the final design for the PD. Of course, also an optimization procedure can be used to automatically select these parameters instead of

Fig. 6 The damper configurations under investigation: (**a**) the tuned mass damper (TMD), (**b**) the particle damper, (**c**) the ballast mass
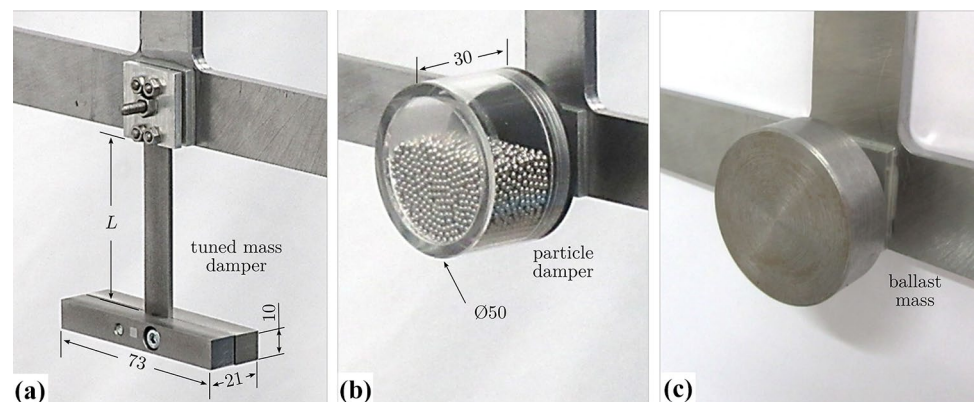
Table 1 Most relevant parameters for the experiments

device	parameter	value
TMD	moving mass (kg)	9.0×10^{-2}
	stiffness (Nm^{-1})	1.56×10^{4}
	beam width (m)	1.2×10^{-2}
	beam length L (m)	5.8×10^{-2}
	beam thickness (m)	2.0×10^{-3}
	beam density (kgm^{-3})	7.85×10^{3}
	total mass (kg)	1.34×10^{-2}
PD	container inner diameter(m)	4.2×10^{-2}
	container inner length (m)	2.1×10^{2}
	particle content mass (kg)	9.4×10^{-2}
	particle radius (m)	1.0×10^{-3}
	particle density (kgm^{-3})	7.85×10^{3}
	fill ratio (-)	60%
	total mass (kg)	1.34×10^{-2}

doing manual variations. The PD consists of a transparent acrylic cylindrical container of inner length 21 mm and an outer diameter of 42 mm. The PD enclosure alone weighs 40 g. Additionally, the PD container is filled with 94 g of spherical steel particles 2mm in diameter. A total of around 2950 steel balls are used. This corresponds to a fill-ratio of

about 60%, see Fig. 6(b). All the relevant PD design parameters are outlined in Table 1.

Influence of PD on the Host-Structure

In order to investigate the influence of a PD on the host structure, the steady state frequency response functions (FRFs) of the three different configurations are measured first. The three configurations are: host structure without a PD, host structure with an added ballast mass (BM) and host structure with a PD. The ballast block is in the same location as the PD and its mass is equal to the static mass of the particle damper. The FRFs for the three configurations are generated by driving the shaker with a frequency sweep signal from 25 to 200 Hz. To make sure that a quasi-steady state is reached, a relatively long frequency sweep time of 500 s is chosen.

Figure 7 shows the frequency response of all three configurations. As expected, it is clearly seen that the added ballast mass does not change the damping properties of the host structure, that is the height of the resonance peaks. The ballast mass merely shifts the resonance frequencies of the host structure to the left, especially the frequencies at 62 Hz and 83 Hz.

The most interesting aspect of Fig. 7 is the influence of the PD on the host structure. Significant damping is

Fig. 7 Experimental frequency response of the host structure without a PD, with an added ballast mass and with a PD. A significant and simultaneous reduction in resonance peaks at multiple eigenfrequencies is observed using a single PD
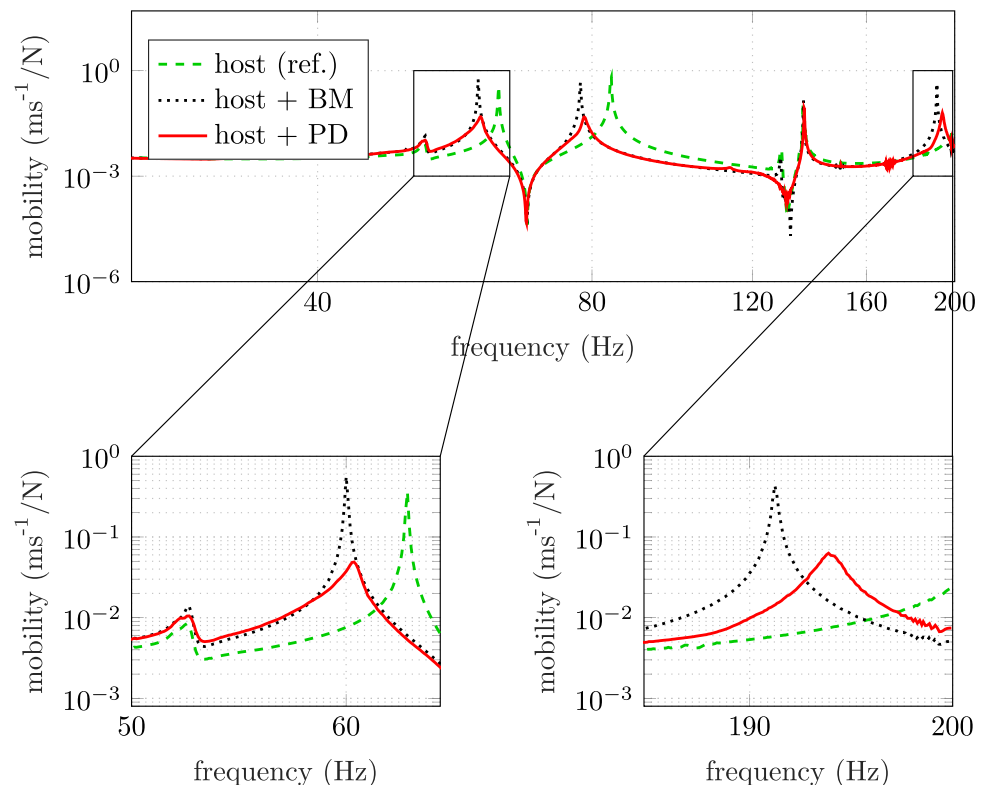
observed in multiple resonance peaks when using a PD. For instance, there is 91.2%, 90%, and 88.78% reduction in the resonance peaks at 60 Hz, 80 Hz, and 190 Hz when using the PD, see the enlargements in Fig. 7. This is a substantial finding since the PD was initially just developed for a design frequency of 60 Hz. However, it exhibits a simultaneous damping effect at multiple frequencies far higher than the design frequency. Another interesting aspect is that the PD does not help in reducing the resonance peaks at 52 Hz and 136 Hz, see Fig. 7(a) and (b). This is because at these frequencies, the PD mounting point is at a vibration node, where the displacement amplitudes are drastically lower, see the mode shapes shown in Fig. 5. Due to much lower amplitudes at these frequencies, there is negligible relative motion between the particles which in turn leads to drastically lower energy dissipation.

Nearly no shift of eigenfrequencies towards the left is observed for the host structure with a PD compared to the one with a ballast mass. The small shift is because some particles within the PD container spend some of their time airborne, resulting in fewer particles in contact with the PD container. As a result, the apparent mass of the PD observed during FRF measurements is lower than its static mass resulting in a slightly lower eigenfrequency shift compared to the ballast mass. The apparent or dynamic mass of the PD not only depends on the excitation parameters (frequency and amplitude), but also depends, in a highly nonlinear way, on many other parameters such as fill-ratio, particle size, shape and material, container geometry among others [10, 21].

Using this experimental study, already two important partial conclusions can be drawn: Firstly, it is demonstrated that a single PD can be deliberately designed to dissipate energy of a relatively complex host structure in a high acceleration amplitude scenario (acceleration higher than 20 times that of gravity). Secondly, it is shown that particle damping is fairly insensitive to the vibration frequency and highly sensitive to the vibration amplitude. Therefore, in order to achieve a calm and smooth frequency response, it is not only important to choose the best PD parameter combination (fill ratio, particle size and shape, materials, inclusion of a liquid, obstacle-grids among others), but also the location of the PD on the host structure should be chosen carefully. That is, the PD should be located where the host structure exhibits maximum vibration amplitudes. It is known that different regimes lead to a different damping behaviour, e.g. sometimes a wild nearly chaotic motion is optimal while sometimes a block like motion of the particles is better, see [22]. Here, a block-like motion of particles (bounding bed) is advantageous.

Particle Damper versus Tuned Mass Damper

Now, the damping performance of a PD is compared to a conventional TMD to see the intrinsic differences in their damping characteristics. The devices which are compared here and the most relevant parameters are shown in Fig. 6 and Table 1, respectively. For the purpose of this study, the host structure with the corresponding damping device is externally excited by providing the shaker with a frequency sweep signal from 25 Hz to 100 Hz within 375 s sweep time. Similar to the investigation in "Influence of PD on the Host-Structure", the host structure with a BM is the reference configuration.

Figure 8 shows the frequency response of the host structure with a TMD, with a PD and with a BM. It is clearly seen that near the design frequency of 60 Hz, the TMD provides superior vibration suppression compared to a PD. This behaviour is expected, because a TMD works by introducing a vibration node at the point of attachment to the host structure exactly at design or operating frequency. Therefore, a conventional TMD actually does not directly dissipate the vibrational energy but rather transfers the energy to the vibration of the attached auxiliary mass. The movement of this mass functions as a kinetic energy reservoir and also leads to dissipation through material damping of the deflected TMD beam, friction in the joints, etc.. Furthermore, a TMD introduces an additional degree of freedom to the host structure and thus, adds additional resonance frequencies. This is clearly seen in the additional resonance peak at 70 Hz for the case where the host structure is fitted with a TMD, see blue dashed curve in Fig. 8(a).

Additionally, the introduction of a TMD lowers the natural frequencies of the reference host structure that are below the design frequencies. For instance, the natural frequency at 60 Hz is now lowered to 45 Hz. On the other hand, the resonance frequencies of the reference host structure that are higher than the design frequency, for instance the frequency at 80 Hz, are raised with the introduction of a TMD, see Fig. 8 for high frequencies. On the whole, the TMD, even though it does a very good job in reducing vibration near the design frequency of 60 Hz, drastically alters the frequency response of the host structure and creates trouble at other frequencies. Another aspect of the TMD is, that its vibration attenuation property is highly sensitive to changes in stiffness and mass of the auxiliary system. In other words, changes in the TMD configuration, for instance due to fatigue, lead to a detuning of the TMD which could result in a sudden unwanted increase in vibrations. Therefore, care has to be taken when designing a TMD and it should only be used for a system that is subjected to a constant frequency excitation.

On the other hand, PDs provide considerable vibration damping not only at 60 Hz but also at other frequencies as discussed in detail in "Influence of PD on the Host-Structure". Unlike a TMD, PDs due to inter particle collisions and friction, actually dissipate the vibrational energy of the host structure and convert it to other energy forms (for instance heat). As seen in Fig. 8, the energy dissipation in the PD is relatively

Fig. 8 Experimental frequency response of the host structure with a BM, TMD and PD. Near the design frequency of 60 Hz, the TMD provides superior vibration attenuation compared to a PD. However, the PD provides considerable vibration damping at multiple resonance frequencies at the same time
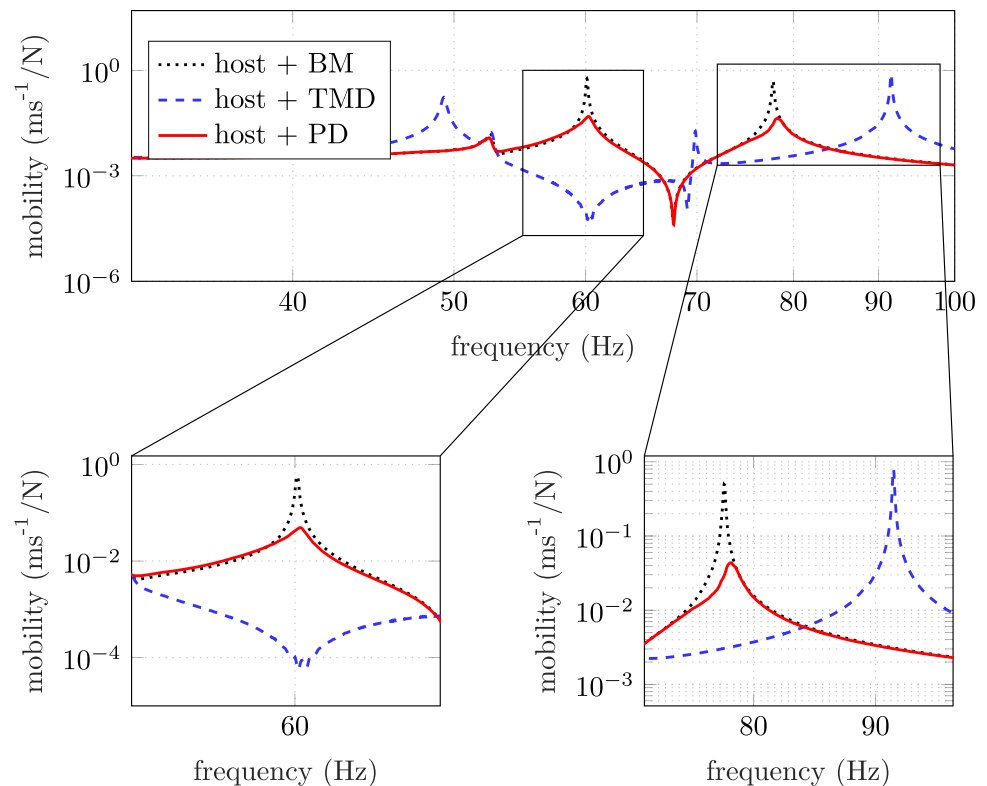
insensitive to the excitation frequency and highly sensitive to the external motion at the attachment point. Consequently, the PD affects the host structure only where the host structure shows high vibration amplitudes and induces no alternation elsewhere, see Fig. 8.

Towards Quantifying Broadband Dissipation

The experimental investigations shown have opened up two crucial questions which are yet to be addressed. To what extent does a particular damping device influence the frequency response of the host structure? Moreover, how can a damping device be rated according to its broadband damping property? In order to answer these questions two additional quantities are introduced.

Firstly, the dynamic influence factor S_{dev} is introduced, which is the ratio of the mobility of the host structure with the damping device to the mobility of the host structure with a ballast block having the same static mass of the device. The factor S_{dev} is defined as

$$S_{dev,f} = \frac{M_{dev,f}}{M_{ref,f}} \quad , \tag{1}$$

where $M_{dev,f}$ is the mobility (velocity/force) of the structure with the damping device at the frequency f and $M_{ref,f}$ is the mobility of the host structure with an equivalent mass block. The factor S_{dev} helps to quantify the effect of the particular

damping device on the host structure. For instance, a high dynamic influence (greater than 1) indicates vibration amplification and a low value (smaller than 1), indicates vibration reduction.

The dynamic influence factor S_{dev} applied to the investigated host structure with a PD and a TMD is shown in Fig. 9. It can be seen that the dynamic influence factor for the TMD has a very low value near the design frequency of 60 Hz, meaning vibration attenuation is only observed around the design frequency. Apart from the design frequency, especially at 49 Hz, 68 Hz, 91 Hz frequencies, the dynamic influence factor for the TMD case has high positive values, indicating even a vibration amplification at these frequencies, i.e. a worsening of the dynamic behaviour. From a practical point of view these vibration amplifications observed only in the TMD case are disadvantageous. This is because the TMD, apart from providing the vibration attenuation at the design frequency, fundamentally alters the frequency response of the host structure elsewhere. Interestingly, the dynamic influence for the PD case is relatively smooth compared to the TMD case. The S_{PD} for the PD case attains values smaller than one (meaning vibration reduction) at frequencies where the host structure exhibits high vibration amplitudes. Usually, the value of S_{PD} is close to one. This means that the PD is a passive damping device which smoothens the resonance peaks without fundamentally altering or shifting the natural frequencies of the host structure.

Fig. 9 Dynamic influence factor computed for the host structure equipped with a PD and a TMD. The S_{PD} shows that the PD influences the host structure only for high vibration amplitudes, whereas S_{TMD} shows that the TMD fundamentally alters the frequency response of the host structure
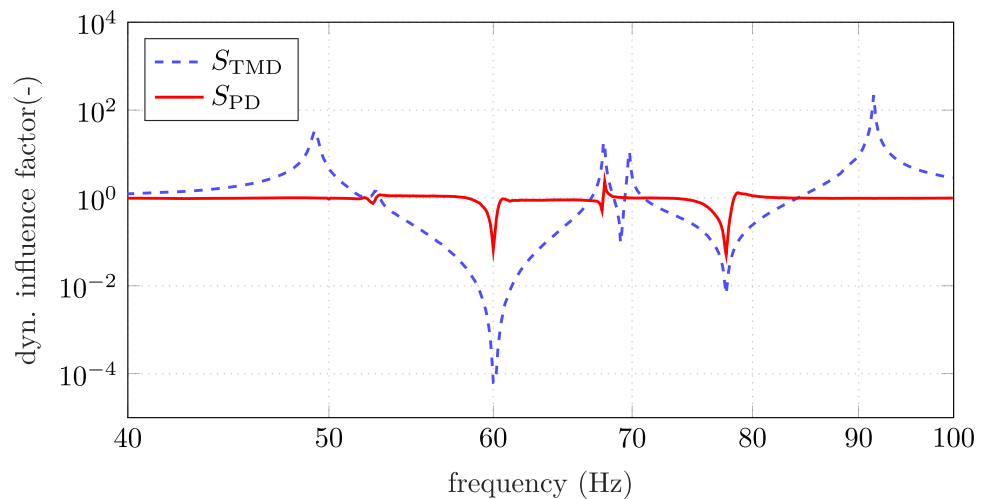
Secondly, to analyse the broadband damping property of a device, another quantity namely the mean influence deviation σ_{dev} is introduced. The deviation σ_{dev} is defined as the squared deviation of the dynamic influence factor from its mean behaviour of a particular damping device. This can be defined as

$$\sigma_{dev,f} = (S_{dev,f} - \bar{S}_{dev})^2 \quad , \tag{2}$$

where $\bar{S}_{dev}$ is the average dynamic influence factor of the host structure equipped with a particular damping device. In other words, σ_{dev} indicates the extent to which a device deviates from its mean response over frequency. A high value of σ_{dev} means, that the device changes its behaviour to a large extent. A perfect broadband damping device would have a value of zero, even though such a device would be impractical. Figure 10 shows the curves for σ_{TMD} and σ_{PD} computed for the host structure equipped with a TMD and PD, respectively. It is clearly seen that the deviation σ_{PD} for the

PD case has a much lower numerical value over the entire frequency range when compared to a TMD. This means that the behaviour of a PD does not drastically deviate from its mean performance compared to a TMD. For the TMD case in can be seen that the vibration amplification around 49 Hz and 91 Hz are prominent in the influence deviation as well. However the attenuation around 60 Hz leads to no observable peak. This is due to numerically small numbers of S_{TMD} from which the constant $\bar{S}_{dev}$ is subtracted. The formulation of $\sigma_{dev,f}$ in equation (2) especially highlights positive deviation from $\bar{S}_{dev}$ which leads to undesired vibration amplification caused by the damping device.

Therefore, the value S_{dev} provides quantitative insights on the extent to which a device influences the host structure and σ_{dev} provides insights regarding the broadband damping property of a damping device. So, S_{dev} and σ_{dev} together provide the right tools to quantitatively investigate damping devices or parameter changes systematically.

Fig. 10 Mean influence deviation computed for the host structure equipped with a TMD and a PD. The σ_{PD} has smaller values compared to σ_{TMD} indicating that the PD does not drastically deviate from its mean behaviour compared to a TMD
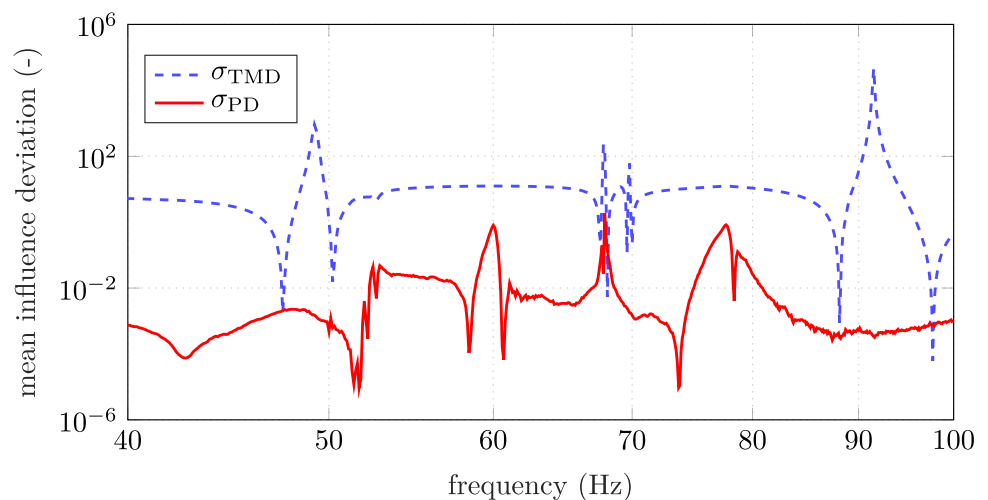
Conclusion

From the experimental investigation conducted in this paper, it can be concluded that a TMD should be used only if the excitation frequency is constant and is know a-priori. For all other cases, where the excitation frequencies are not known, a PD with its proven wide band damping capability provides a viable alternative. The accomplished percental reduction of the PD almost matches that of the TMD for its tuning frequency. Additionally the PD also reduces the vibration amplitudes for all other eigenfrequencies. In the experimental investigations shown here, the steady state response of the host structure with a PD is considered. This allows an independent evaluation of the influence at different frequencies. Therefore, a harmonic frequency sweep signal with a relatively low frequency sweep rate is used. The defined performance metrics give a descriptive for broadband damping properties of a damping device. This is a basis for problem specific handling of these broadband characteristics.

Declarations

Ethical Approval No animal or human subjects were used in this research.

Conflicts of Interest All authors declare to have no conflicts of interest.

References

1. Popplewell N, Semercigil S (1989) Performance of the bean-bag impact damper for a sinusoidal external force. J Sound Vib 133(2):193–223

2. Friend RD, Kinra VK (2000) Particle impact damping. J Sound Vib 233:93–118

3. Marhadi KS, Kinra VK (2005) Particle impact damping: effect of mass ratio, material, and shape. J Sound Vib 283:433–448

4. Gnanasambandham C, Schönle A, Eberhard P (2019) Investigating the dissipative effects of liquid-filled particle dampers using coupled DEMSPH methods. Computational Particle Mechanics 6:257–269

5. Tomlinson G, Pritchard D, Wareing R (2001) Damping characteristics of particle dampers - some preliminary results. Proc Inst Mech Eng C J Mech Eng Sci 215(3):253–257

6. Li X, Yang Y, Shi W (2019) Study on the damping effect of particle dampers considering different surface properties. Shock Vib 2019:8293654

7. Liu W, Tomlinson G, Rongong J (2005) The dynamic characterisation of disk geometry particle dampers. J Sound Vib 280:849–861

8. Gnanasambandham C, Eberhard P (2019) Modeling a partially liquid-filled particle damper using coupled Lagrangian methods. International Centre for Numerical Methods in Engineering (CIMNE), Barcelona

9. Bannerman MN, Kollmer JE, Sack A, Heckel M, Mueller P, Pöschel T (2011) Movers and shakers: granular damping in microgravity. Phys Rev E84:011301

10. Gagnon L, Morandini M, Ghiringhelli G (2019) A review of particle damping modeling and testing. J Sound Vib 459:114865

11. Zhang K, Chen T, He L (2017) Damping behaviors of granular particles in a vertically vibrated closed container. Powder Technol 321:173–179

12. Meyer N, Seifried R (2021) Damping prediction of particle dampers for structures under forced vibration using effective fields. Granul Matter 23, Art. 64

13. Fowler B, Flint E, Olson S (2012) Effectiveness and predictability of particle damping. Smart Structures and Materials 2000: Damping and Isolation 3989:13

14. Panossian H (1992) Structural damping enhancement via non-obstructive particle damping technique. J Vib Acoust 114:101–105

15. Wang D, Wu C (2015) Parameter estimation and arrangement optimization of particle dampers on the cantilever rectangular plate. Journal of Vibroengineering 17(5):2503–2520

16. Aubert AC, Green ER, Chen GZ (2003) A comparison of the effectiveness of elastomeric tuned mass dampers and particle dampers. In: SAE 2003 Noise & Vibration Conference and Exhibition. SAE International

17. Lu Z, Huang B, Wang Z (2018) Experimental comparison of dynamic behavior of structures with a particle damper and a tuned mass damper. J Struct Eng 144

18. Lu Z, Wang D, Li P (2014) Comparison study of vibration control effects between suspended tuned mass damper and particle damper. Shock Vib 2014:903780

19. Knaebel M (1992) Technische Schwingungslehre (in German). Teubner, Stuttgart

20. Gnanasambandham C, Fleissner F, Eberhard P (2020) Enhancing the dissipative properties of particle dampers using rigid obstacle-grids. J Sound Vib 484:115522

21. Lu Z, Wang Z, Masri SF, Lu X (2017) Particle impact dampers: past, present, and future. Struct Control Health Monit 25:1–25

22. Lu Z, Wang Z, Zhou Y, Lu X (2018) Nonlinear dissipative devices in structural vibration control: a review. J Sound Vib 423:18–49

Publisher's Note Springer Nature remains neutral with regard to jurisdictional claims in published maps and institutional affiliations.